


# The STAT3/NFIL3 signaling axis-mediated chemotherapy resistance is reversed by Raddeanin A via inducing apoptosis in choriocarcinoma cells

Zheng Peng | Chun Zhang | Wenjun Zhou | Chenchun Wu | Yi Zhang 

Department of Gynecology and Obstetrics, Xiangya Hospital of Central South University, Changsha, China

## Correspondence

Yi Zhang, Department of Gynecology and Obstetrics, Xiangya Hospital of Central South University, Changsha 410008, China.  
Email: zhangyi5588@csu.edu.cn

## Funding information

Graduate Independent Innovation Project Fund of Central South University, Grant number: 2016zsts125

Chemotherapy resistance is the major issue of choriocarcinoma. Apoptosis always is the ultimate outcome of chemotherapeutic drugs, which considered one of the reasons of resistance. We investigated the role of STAT3/NFIL3 signaling-inhibited apoptosis in chemotherapy resistance and whether Raddeanin A (RA) could be a new drug to reverse resistance. Established three drug-resistant cell lines as JEG-3/MTX, JEG-3/5-FU, and JEG-3/VP16. NFIL3 and STAT3 expression was evaluated in the cells. The IC<sub>50</sub> value, apoptosis rate and apoptins were observed with transfection of siNFIL3, Lenti-OE™-NFIL3, shSTAT3, and Lenti-OE™-STAT3 or RA treatment. In addition, the luciferase reporter analysis and co-immunoprecipitation assays were used to investigate the relation of STAT3 and NFIL3. Hyper-activation of STAT3 and NFIL3 expression were observed in three drug-resistant cell lines. STAT3 enhanced NFIL3 transcriptional activity by binding the relative promoter region. Activated STAT3/NFIL3 pathway caused low rate of apoptosis which resulted in chemotherapy resistance. RA reduced the resistance index of resistant cells and induced caspase 3 dependent apoptosis, meanwhile it repressed the STAT3/NFIL3 activation. STAT3/NFIL3 axis-inhibited apoptosis is a novel mechanism of chemotherapy resistance in choriocarcinoma. With the suppression of STAT3/NFIL3 axis and apoptosis induction, RA is a potential agent or lead candidate for improving chemotherapy.

## KEYWORDS

apoptosis, chemotherapy resistance, NFIL3, Raddeanin A, STAT3

## 1 | INTRODUCTION

Choriocarcinoma (CC) is one of the gestational trophoblastic neoplasias (GTNs), which is characterized by human chorionic gonadotropin (hCG) elevation as a malignant lesion often arising in childbearing years women (Lurain, 2011). The overall cure rate in the CC is currently about 80%, which is the result of the inherent sensitivity to chemotherapy (Seckl et al., 2013).

However, parts of these develop drug resistance in the chemotherapy, which result in reduction of therapeutic effect, leading to metastatic lesion or adding risk of hysterectomy, and loss of fertility (Chen et al., 2007). It is important to investigate the mechanism responsible for resistance and discover new drugs reversing drug resistance.

One model that has received considerable attention in last years relates with the acquisition of resistance to chemotherapy by

This is an open access article under the terms of the Creative Commons Attribution-NonCommercial-NoDerivs License, which permits use and distribution in any medium, provided the original work is properly cited, the use is non-commercial and no modifications or adaptations are made.

© 2017 The Authors. *Journal of Cellular Physiology* Published by Wiley Periodicals Inc.

suppressed-apoptosis (Rathore, McCallum, Varghese, Florea, & Büsselberg, 2017). Importantly the high level of apoptosis was observed in methotrexate-resistant JEG-3 cells compared with parental cells (Shen et al., 2015). Indeed, we also found that there were different levels of apoptosis variation in drug-resistant CC cells in preliminary experiment. Hence, we hypothesized that apoptosis inhibition may contribute to the development of drug resistance.

NFIL3 (nuclear factor interleukin 3 regulated, also known as E4 binding protein 4, E4BP4) impacts many cellular processes and is widely expressed in human tissues, especially could highly induced by hCG treatment (Kashiwada, Pham, Pewe, Harty, & Rothman, 2011; Li, Liu, & Jo, 2011). Apoptosis plays a major role in development and tissue homeostasis (Fuchs & Steller, 2011; Lim, Yang, Bazer, & Song, 2017). NFIL3 could inhibits apoptosis in numerous settings from B-cells to motor neurons, which 50% undergo apoptosis (Ikushima et al., 1997). High-expression of NFIL3 in embryonic rat and chicken motor neurons that survive developmental pruning, while more than half of the motor neurons produced undergo programmed cell death (Raff et al., 1993). In line with its ability to hinder cell death, NFIL3 has emerged as a novel survival factor in cancer. In the research of mechanisms in IL-10-mediated anti-inflammatory effect, it is found that NFIL3 is a key component of the STAT3-mediated anti-inflammatory mechanism (Smith et al., 2011). Signal transducer and activator of transcription 3 (STAT3) belongs to STAT family of proteins. Constitutively active STAT3 mediates critical gene expression changes and molecular events that regulating cell growth and apoptosis (Turkson & Jove, 2000; Yang et al., 2012). As a now validated anticancer drug target, the inhibitors of the STAT3 pathway as a novel approach to inducing cancer cell apoptosis and hence treating cancer patients (Niu et al., 2011; Zhang, Zhou, Gu, Yan, & Zhang, 2014). But the clinical safety of these compound is not clear, investigation of new usage in traditional drugs is more popular.

Several traditional Chinese medicines are used for the treatment of tumors including gynecological carcinomas in China. Raddeanin A (RA) is an oleanane-type triterpenoid saponin extracted from the root of *Anemone raddeana* Regel, a traditional Chinese medicinal herb (Luan et al., 2013). The mainly functions of RA which once reported are developed to anti-inflammation and anti-tumor treatments (Guan et al., 2015). Previous studies have also shown that RA induced apoptosis and inhibited invasion in human gastric cancer cells (Xue et al., 2013). And in our preliminary studies, RA can suppress choriocarcinoma JEG-3 cells proliferation (unpublished data). More importantly, RA showed synergy with cisplatin in therapeutic effect in human hepatocellular carcinoma (Li et al., 2017). However, its effect and mechanisms on drug resistance are still largely unknown. In this study, the possible mechanisms of resistance, and the inhibitory effects of RA on the reversal resistance of chemotherapeutics in CC were investigated.

## 2 | MATERIALS AND METHODS

### 2.1 | Drug and cells

Raddeanin A was obtained from National Institute for the Control of Pharmaceutical and Biological Products (Beijing, CN). The human

choriocarcinoma JEG-3 cell line was laboratory-preserved which purchased from the American Type Culture Collection (ATCC, Manassas, VA) (Shi, Tan, Lu, Yang, & Zhang, 2014). Anti-etoposide cell line named JEG-3/VP16 was purchased from the China Center for Type Culture Collection (Wuhan, China). Cells were cultured in DMEM-high glucose supplemented (Gibco, Rockford, IL) with 10% FBS (Gibco), 50 U/ml penicillin, and 50 µg/ml of streptomycin at 37 °C in a 5% CO<sub>2</sub> atmosphere.

### 2.2 | Establishment of drug-resistant sublines

Methotrexate (MTX)- and fluorouracil (5-FU)-resistant variants were obtained by exposing parental cell line to stepwise increased MTX and 5-FU (Sigma, St. Louis, MO) concentrations by intermittent- and consecutive-feeding methods (Snow & Judd, 1991). The JEG-3/MTX obtained by initially exposing JEG-3 from 0.001 to 10 µg/ml MTX until they achieved a growth rate like untreated cells. The JEG-3/5-FU was the same, whereas they exposed in the 5-FU concentration from 0.025 to 50 µg/ml.

### 2.3 | Cell proliferation assay

The inhibitory concentration 50% (IC<sub>50</sub>) was explored with Cell Counting Kit-8 (Dojindo, Kumamoto, JPN) assay as per the protocols. Total of  $2 \times 10^4$  all four kinds of cells were seeded into 96-well plates with approximately 80% cellular fusion. Then cells were treated with drugs for 48 hr, each well was added 10 µl CCK-8 for 2 hr at 37 °C. The absorbance was measured at 450 nm with a microplate reader (BioTek, Winooski, VT). Resistance Index (RI) = IC<sub>50</sub> of the drug-resistant cells/IC<sub>50</sub> of the parent cells.

### 2.4 | Flow cytometric analysis for apoptosis

To analyze cell apoptosis, cells with varies treatments were stained by propidium iodide (PI) and FITC-Annexin V as the Apoptosis Detection Kit (BD, Franklin Lakes, NJ) protocol, tested by Flow Cytometer (BD). The results analyzed by FlowJo software.

### 2.5 | TUNEL assay

The cell TUNEL assay was performed using Apoptosis Detection Kit (Roche, Basel, CH) as the protocol. Briefly, Total  $3 \times 10^4$  cells were planted in six-well plate with various treatments for 24 hr. The treated adherent cells were fixed in 4% paraformaldehyde for 15 min, then treated with TritonX-100 for 15 min. Cells in every well were incubated with 50 µl TUNEL reaction solution (5 µl TdT +45 µl dUTP) in a humidified box at 37 °C for 1 hr. POD-horseradish peroxidase incubated cells for 30 min, then colorized with DAB. The positive cells with green fluorescence was counted under a fluorescence microscope (Leica, Wetzlar, DE). Five high power microscopic views (×200) were chosen on each slide.

## 2.6 | RNA extraction and real-time polymerase chain reaction (RT-PCR)

Total RNA was extracted using the TRIzol reagent (Life Technologies, Rockford, IL) following the manufacturer's instruction. cDNA was reversely transcribed by a Transcriptor First Strand cDNA Synthesis Kit (Life Technologies). RT-PCR was performed using SYBR PremixEx Taq™ II (Life Technologies) with ABI 7500 real-time PCR system (Thermo, MMAS, Rockford, IL). The expression level was calculated with  $2^{-\Delta\Delta Ct}$  versus control group. The primers sequences were listed in Supplementary Table S1.

## 2.7 | Western blot analysis

Total proteins were extracted by RIPA lysis buffer (Beyotime biotechnology, Shanghai, CN) and quantified with the standard BCA method. Equivalent amounts of protein from each sample (30–50 µg) were loaded onto an SDS-PAGE gel and transferred onto PVDF membranes (Merck, Darmstadt, DE). TBST supplemented with 5% milk was used for blocking the membrane for 1 hr at room temperature, and then incubated with various primary antibodies (all the primary antibodies were purchased from CST, Darmstadt, DE; Phospho-Stat3 (Tyr705)#9415, STAT3#9136, NFIL3#14312, Cleaved Caspase-3#9664, Caspase-3#9662, Bcl-2#4223) at 4 °C overnight with gently shaking. Secondary antibodies (CST, Darmstadt, DE) were added for 1 hr and detected with ECL reagent (Millipore, Billerica, MA), and exposed by chemiluminescence system (Syngene, Cambridge, UK). The gray value of each band was measured by ImageJ software.

## 2.8 | Transfection

The scramble, NFIL3 siRNA (5'-GAUGAGGGUGUAGUGGGCAAGU-CUU-3') were synthesized by Ribobio (Guangzhou, CN). Cells were seeded in six-well plates with a density of  $2 \times 10^5$  cells/well and transfected with siRNAs using the riboFECT™ CP (Ribobio, Guangzhou, CN). The LV-STAT3-RNAi was provided by Open Biosystems (RMM3981-97059843, clone ID TRCN0000071456). The over-expression Lenti-OE™-STAT3 and Lenti-OE™-NFIL3 were provided by Genechem (Shanghai, CN), which transfected into cells for 48 hr.

## 2.9 | Luciferase reporter assay

The NFIL3 promoter including the wild STAT3-NFIL3 binding sites or mutant type was cloned into the pGL3-Basic vector (Ribobio, Guangzhou, China). The luciferase reporter assay (Promega, Madison, WI) executed following the luciferase reporter assay protocol. JEG-3 cells were co-transfected with reporter plasmid (pGL3-NFIL3 wt/mt), STAT3, shSTAT3, or treated with 50 ng/ml IL-6 (Sigma) treatment as indicated. The fluorescence value was detected by GloMax-multimode reader (Promega).

## 2.10 | Co-immunoprecipitation

The total protein was lysed in RIPA lysis buffer, and then was incubated with anti-pSTAT3 or IgG as a negative control. Added to agarose shaken for 4 hr at 4 °C and centrifuged for 5 min at 2,500g following. The washed precipitation was suspended in SDS buffer with primary antibodies against p-STAT3 and NFIL3, used for Western blot analyses.

## 2.11 | Bioinformatic data mining

We downloaded GEO data of different resistant cells from GEO DataSedts (<https://www.ncbi.nlm.nih.gov/gds/>) as our samples of correlation analysis. The molecular functional network map of canonical pathways including co-expression, co-localization, genetic interactions, pathway, physical interactions, predicted networks of NFIL3 analyzed by GeneMANIA (<http://genemania.org/>).

## 2.12 | Statistical analysis

Statistical analysis was performed using SPSS 17.0 software. The datas expressed as the mean ± standard deviation. One-way ANOVA test was used to examine the statistical difference of datas between the groups. Spearman correlation analysis was used to test the co-expression correlation of STAT3 and NFIL3. The significance was defined as *p*-values <0.05.

# 3 | RESULT

## 3.1 | Low rate of apoptosis in drug-resistant cells

To identify factors that contribute to the development of chemotherapeutics-resistance in CC cells, besides the JEG-3/VP16, we performed serial culturing to establish other two resistant sublines of JEG-3 cells, which was named JEG-3/MTX and JEG-3/5-FU. After almost 10 months drug induction, we got resistant cells as Figure 1a shows. CCK-8 assay used in investigating the chemosensitivity. As representatively demonstrated in Figure 1b, the resistant cells all showed higher IC<sub>50</sub> against JEG-3 cells. Exposing the methotrexate, the JEG-3/MTX cells exhibited a mean IC<sub>50</sub> of 32.53 µg/ml while the JEG-3 cells exhibited a mean IC<sub>50</sub> = 1.156 µg/ml (*p* < 0.01). In JEG-3/5-FU cells, the JEG-3/5-FU cells exhibited a mean IC<sub>50</sub> of 196.530 µg/ml while the JEG-3 cells exhibited a mean IC<sub>50</sub> = 6.418 µg/ml (*p* < 0.01). Finally, in JEG-3/VP16 cells exhibited a mean IC<sub>50</sub> = 73.079 µg/ml while the JEG-3 cells exhibited a mean IC<sub>50</sub> = 2.448 µg/ml (*p* < 0.001). Consistently, the resistant cells showed more than 20-fold resistance against parent cells. After repeated experiments, we found that the three sublines showed a low rate of apoptosis exposing chemotherapeutics using Flow cytometry (Figure 1c) and TUNEL (Figure 1d) assay detecting. Then, the apoptins changed in the chemotherapeutic-induced apoptosis were observed (Figure 1e). Whether the parent cells or derivate cells, the caspase 3 pathway was activated similarly. The anti-apoptosis protein Bcl-2 level was increased reversely.

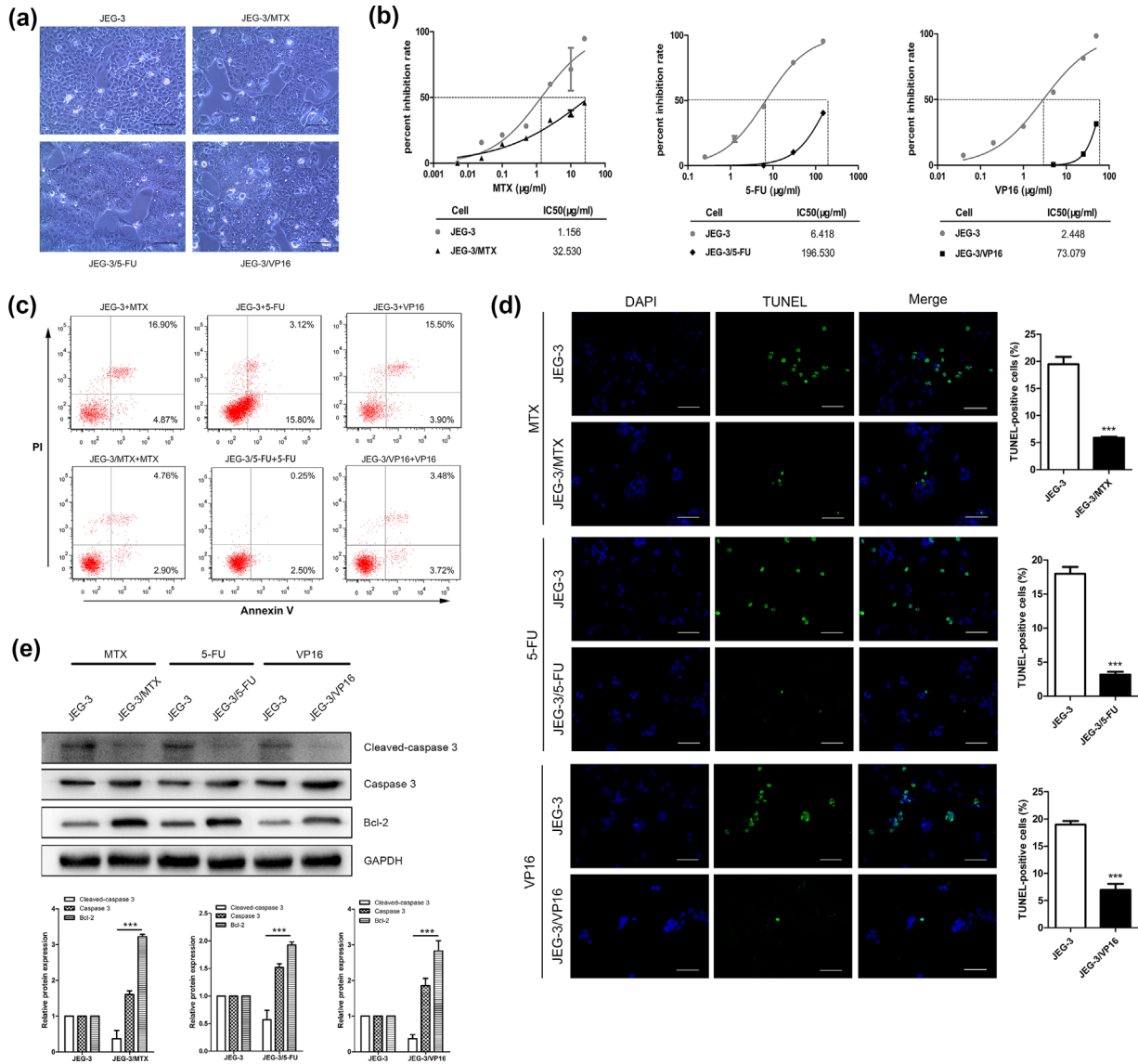


**FIGURE 1** Low rate of apoptosis in drug-resistant cells. (a) The cell morphology of four cells, scale bars 200 μm. (b) IC<sub>50</sub> dose response curves of methotrexate, fluorouracil, and etoposide in three sublines versus JEG-3 cells. (c) Representative flow cytometry images of annexin V/PI-stained four cell lines treated with drugs for 24 hr. (d) Representative images of TUNEL-stained cells treated with chemotherapeutics for 24 hr, blue DAPI-stained nuclei, green TUNEL-stained positive nuclei, scale bars 100 μm (left). Respective TUNEL-positive cells are depicted as percent (right). (e) Cleaved-Caspase 3, Caspase 3 and Bcl-2 protein level in cells treated with chemotherapeutics for 24 hr. GAPDH was used as the internal control (above). Respective changes in protein levels are depicted as fold change (under). Data represent mean ± SD from at least three independent experiments, \*\*\**p* < 0.001

### 3.2 | NFIL3 represses drug-induced apoptosis

In the procession of establishment of drug-resistant cells, NFIL3 protein level highly increased as cultivating generation (Figure 2a) with chemotherapeutics. We hypothesized that NFIL3 related to the formation of drug resistance. To test it, cells transfected with NFIL3 siRNA was established. As the Figure 2b showed, the IC<sub>50</sub> of chemotherapeutics was significantly decreased in the siNFIL3 group compared with controls (mock group; *p* < 0.001). To study whether NFIL3 repressed chemotherapeutics-induced apoptosis in CC cells, TUNEL (Figure 2c) and Flow cytometry (Figure 2d) were used. The siNFIL3 group exposed in drugs for 24 hr, with a higher apoptosis rate than the NC-treated cells (*p* < 0.001).

### 3.3 | Activated STAT3 signaling enhances NFIL3 promoter activity

Aberrant IL-6/STAT3 signaling in cancer cells have emerged as a major mechanism for cancer initiation and development. IL-6 can induces STAT3 activation (Yu & Jove, 2004), what is no exception in the drug-resistant CC cells (Supplementary Figure S1). We performed a detailed analysis of the NFIL3 promoter in the NCBI database, and identified the main STAT3-binding sites (Figure 3a). Luciferase reporter vectors containing wild type and mutant type were constructed and subjected to luciferase reporter assay. The relative luciferase activity was significantly decreased with transfection of shSTAT3, but it was increased by STAT3 overexpression and IL-6 stimulation (Figure 3b).

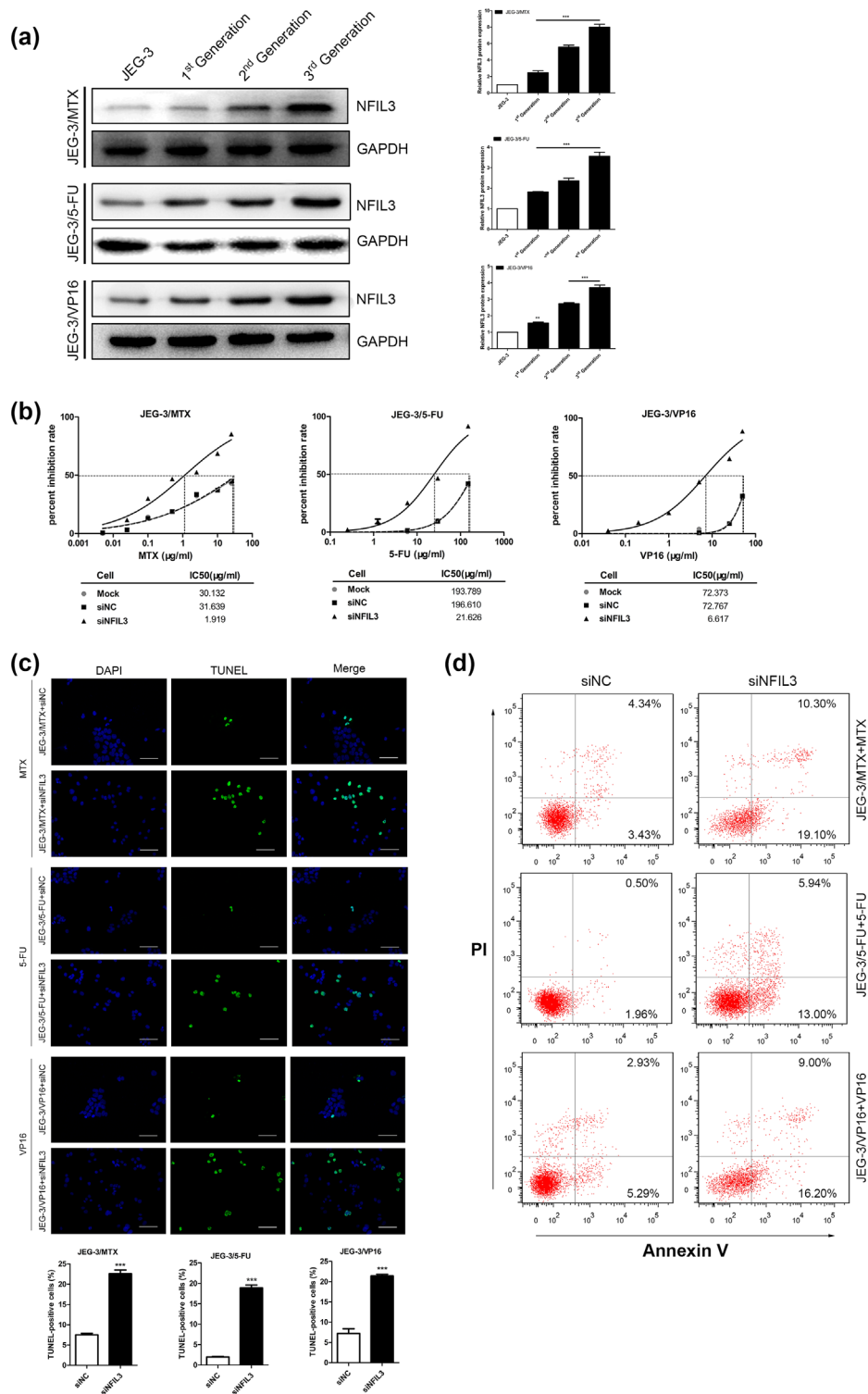


**FIGURE 2** NFIL3 represses drug-induced apoptosis. (a) Western blot analysis of NFIL3 protein levels in different generations of subline cells (left) and subsequent densitometric quantification (right; top to bottom are JEG-3/MTX, JEG-3/5-FU, and JEG-3/VP16). Changes in protein levels are represented as fold change comparison with JEG-3 cells. (b) The IC<sub>50</sub> dose response curves of Mock, NC-treated, and siNFIL3-treated in all subline cells tested in vitro. (c) Representative images of TUNEL-stained cells treated with siNFIL3 or NC control, and then exposed to drugs for 24 hr. Blue DAPI-stained nuclei, green TUNEL-stained positive nuclei, scale bars 100 µm (above). Respective TUNEL-positive cells are depicted as percent (under). (d) Cells were exposed to chemotherapeutics for 24 hr after Annexin V-FITC/PI staining flow cytometry analysis was performed. Representative data are shown from three independent experiments. \*\* $p < 0.01$ , \*\*\* $p < 0.001$



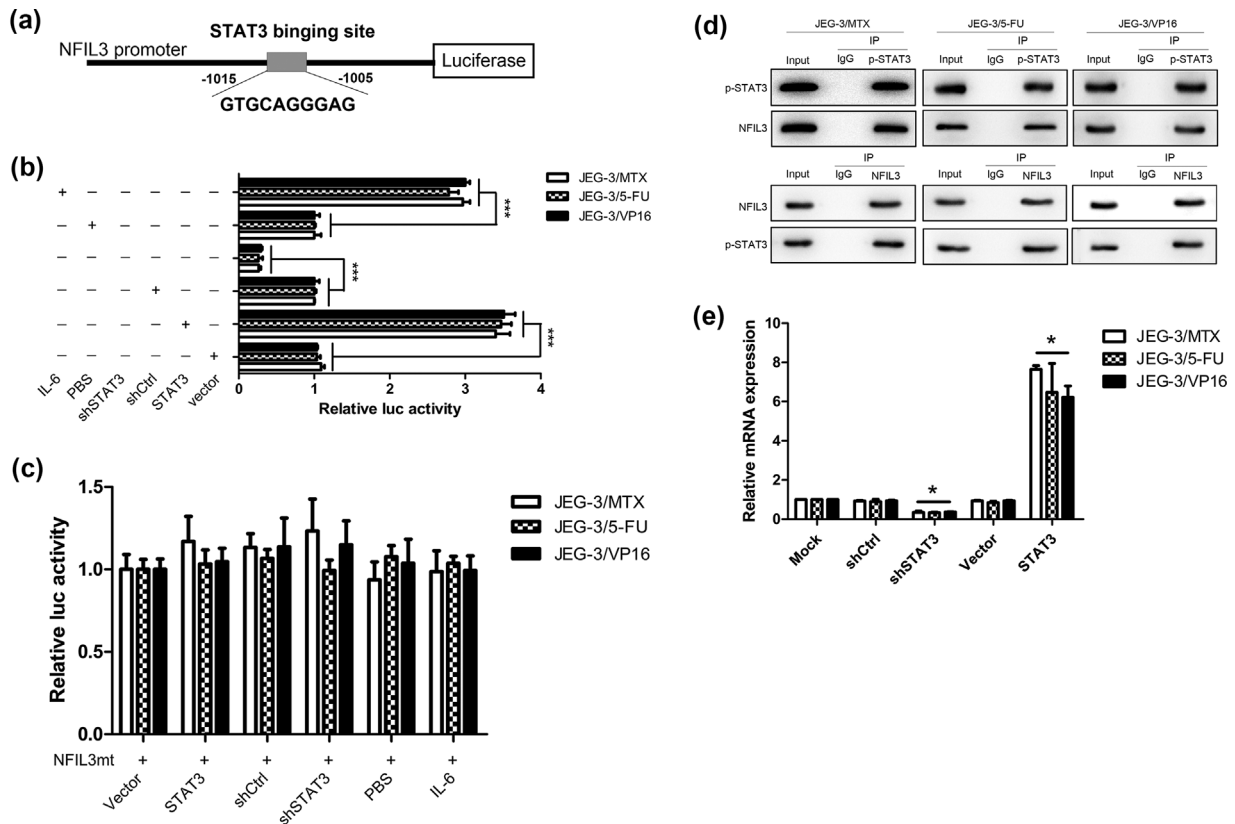


**FIGURE 3** Activated STAT3 signaling enhances NFIL3 promoter activity. (a) Details of STAT3-binding site in NFIL3 promoter. (b) Luciferase assays were performed in three cell lines transfected with STAT3, shSTAT3, or treated with IL-6. (c) Luciferase assays were performed using mutant NFIL3 promoter. (d) Co-immunoprecipitation assays showed that p-STAT3 interacts with NFIL3 in three cell lines respectively. (e) NFIL3 mRNA expression was regulated in three cell lines transfected with shSTAT3 or STAT3 overexpression lentivirus. The results were presented as mean  $\pm$  SD ( $n = 3$ ). \* $p < 0.05$ , \*\*\* $p < 0.001$

And the luciferase activity of reporter vector containing mutant type of STAT3-binding site was unaltered by STAT3, shSTAT3, or IL-6, suggesting that STAT3 enhances NFIL3 induced transcription activation via the site (Figure 3c). Moreover, the stimulation of IL-6 indeed enhanced only STAT3 in CC. Then, we examined whether STAT3 could form complexes with NFIL3 in drug-resistant cells using co-immunoprecipitation assay. As shown in Figure 3d, activated STAT3 interacts with NFIL3 in three cell lines. Further, STAT3 RNAi decreased the level of NFIL3 expression and the overexpression STAT3 increased NFIL3 mRNA (Figure 3e) and protein expression (Figure 4e) level inversely.

### 3.4 | Co-expression of STAT3 and NFIL3 correlated with chemotherapy resistance

As the same of NFIL3, STAT3 was activated as cultivating generation (Figure 4a). We performed a rescue experiment in resistant cells by transfecting LV-STAT3-RNAi. As the Figure 4b showed, the IC<sub>50</sub> of chemotherapeutics was significantly decreased in the shSTAT3 transfected cells compared with controls (mock group;  $p < 0.001$ ). At the same time, LV-STAT3-RNAi increased the apoptotic rate subjected to chemotherapeutics which tested by TUNEL assay (Figure 4c) and Flow cytometry analysis (Figure 4d). Meanwhile,

Caspase 3 dependent apoptosis pathway was activated by shSTAT3 (Figure 4e). All above, activated STAT3 can affect the chemotherapeutic resistance by repressing apoptosis. The mechanism which STAT3 regulated during apoptosis is unknown. As the present study had confirmed STAT3 can regulate NFIL3 in CC cells, we hypothesized that STAT3 mediated apoptosis through regulating NFIL3 expression. As Figure 4e Western blot showed, no matter shSTAT3 or siNFIL3 can increased cells apoptosis rate exposing drugs, but importantly the NFIL3 overexpression offset the apoptotic effect of shSTAT3. In addition, co-transfection with shSTAT3 and siNFIL3 cells showed higher apoptosis stage.

Due to the less data of choriocarcinoma, we performed separately for methotrexate-, fluorouracil- and etoposide-resistant cells in different tumor using GEO DataSets. Results showed that the expression of STAT3 and NFIL3 were highly correlated whether in which one chemotherapeutic (Figure 5a-c). To further observe the possible molecular pathway of NFIL3 and STAT3, the online GeneMANIA tool was used. The networks identified by GeneMANIA are shown in Figure 5d. We observed some genes related with both STAT3 and NFIL3 directly, listed in Supplementary Table S2. Together these results indicate the co-expression of STAT3 and NFIL3 correlate with chemotherapy resistance.

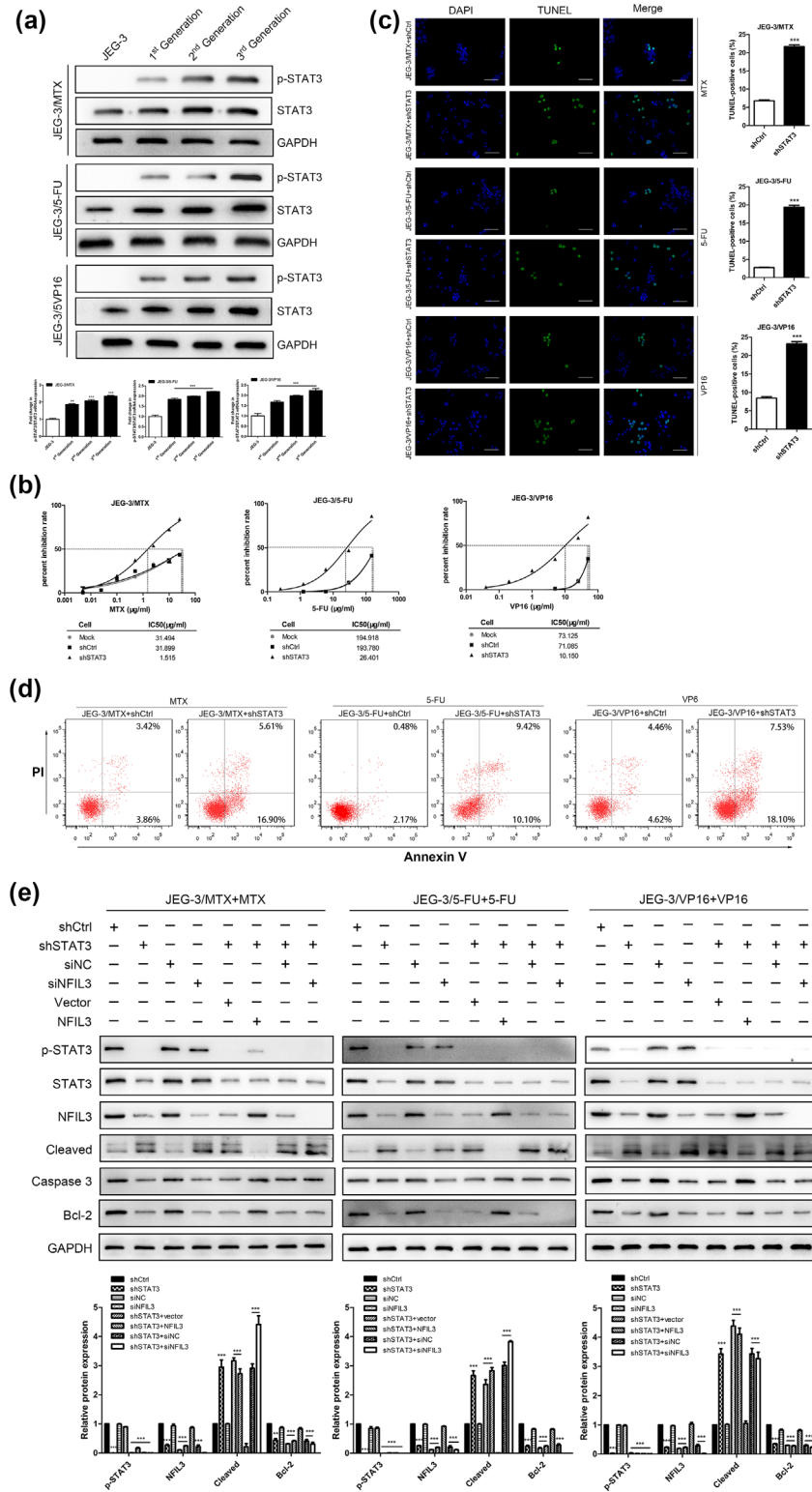


**FIGURE 4** Co-expression of STAT3 and NFIL3 correlated with chemotherapy resistance. (a) Western blot analysis of STAT3 protein levels in different generations of subline cells (above) and subsequent densitometric quantification changes in protein levels are represented as fold change comparison with JEG-3 cells (under). (b) The IC<sub>50</sub> dose response curves of Mock, NC-treated and siNFIL3-treated in all subline cells tested in vitro. (c) Representative images of TUNEL-stained cells treated with shSTAT3 or NC control, and then exposed to chemotherapeutics for 24 hr. Blue DAPI-stained nuclei, green TUNEL-stained positive nuclei, scale bars 100  $\mu$ m (left). The Respective TUNEL-positive cells are depicted as percent (right). (d) Cells were exposed to chemotherapeutics for 24 hr after Annexin V-FITC/PI staining flow cytometry analysis was performed. (e) p-STAT3, STAT3, NFIL3, Cleaved-Caspase 3, Caspase 3, and Bcl-2 protein levels in cells treated with chemotherapeutics for 24 hr. GAPDH was used as the internal control (above). Respective changes in protein levels are depicted as fold change (under). Representative data are shown from three independent experiments. \*\* $p < 0.01$ , \*\*\* $p < 0.001$

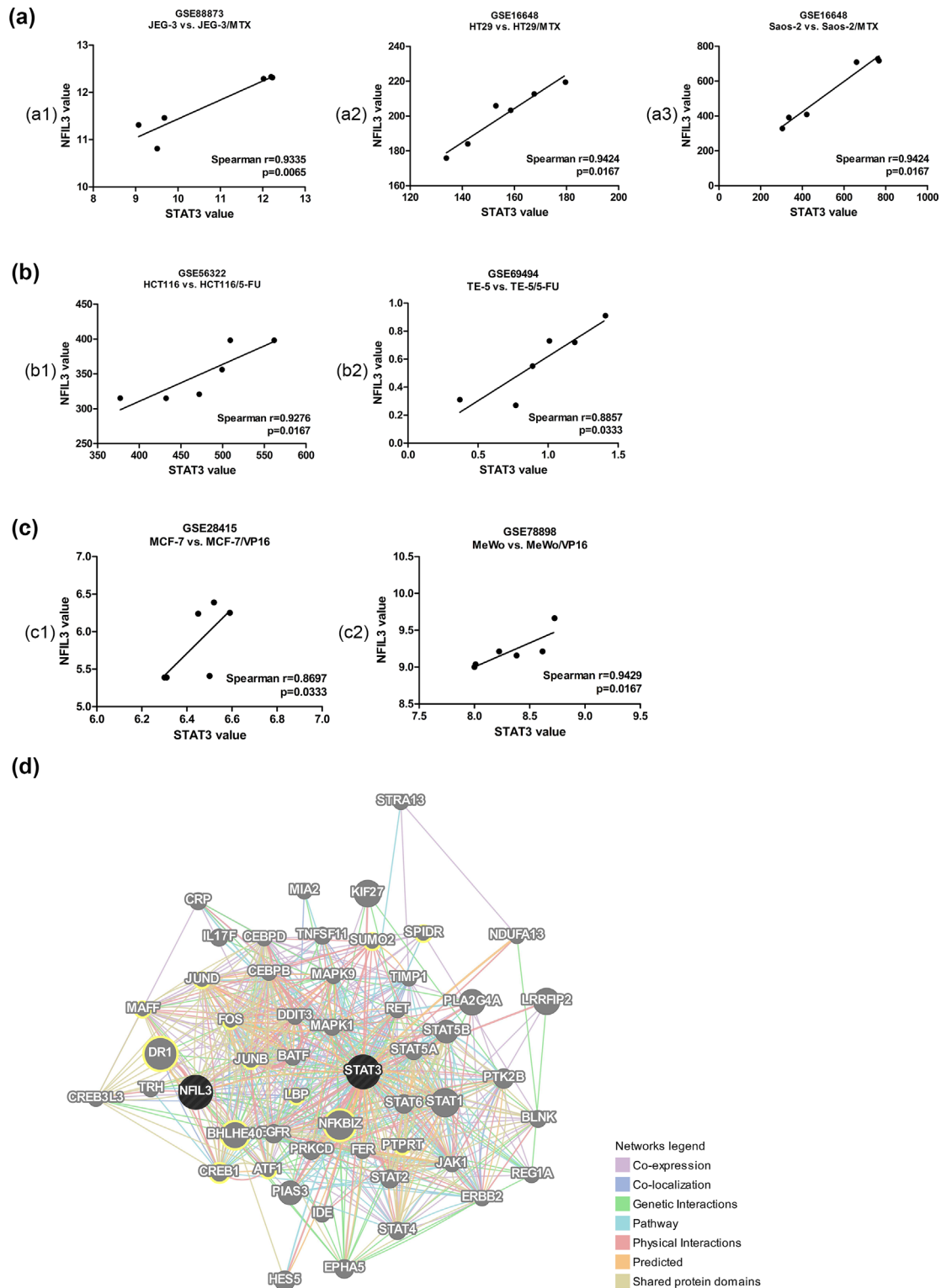


**FIGURE 5** NFIL3 expression positively correlates with the levels of STAT3. (a) NFIL3 and STAT3 mRNA expression levels in methotrexate-resistant cells versus parent cells. (a1) for choriocarcinoma JEG-3 cells in GSE88873; (a2) for colon cancer HT29 cells in GSE16648; (a3) for osteosarcoma Saos-2 cells in GSE16648. (b) NFIL3 and STAT3 mRNA expression levels in fluorouracil-resistant cells versus parent cells. (b1) for colon cancer HCT116 cells in GSE56322; (b2) for esophageal cancer TE-5 cells in GSE69494. (c) NFIL3 and STAT3 mRNA expression levels in etoposide-resistant cells versus parent cells. (c1) for breast cancer MCF-7 cells in GSE28415; (c2) for malignant melanoma MeWo cells in GSE78898. (d) The molecular functional network map of NFIL3 and STAT3 analyzed by GeneMANIA tool



### 3.5 | Raddeanin A induced apoptosis to reverse drug resistance

The chemical structure of RA showed as Figure 6a. Given the drug-resistant cells showed a low rate of apoptosis which related with drug tolerance, to further confirm RA's induction of cell apoptosis, western blot was applied to analyze the apoptosis-related molecules. Cells were treated by three different dosages RA for 24 hr and the results showed that the Cleaved-Caspase 3, Bcl-2 levels changed significantly in a dose-dependent manner (Figure 6b). Cells were treated with the maximal dose 8  $\mu$ M RA we used for 24 hr beforehand, and then exposing to methotrexate, fluorouracil or etoposide before analyzed by TUNEL assay (Figure 6c) and flow cytometric (Figure 6d). The apoptosis rate increased from 6.32% to 53% (JEG-3/MTX,  $p < 0.001$ ), from 2.25% to 56.1% (JEG-3/5-FU,  $p < 0.001$ ), and from 7.51% to 47.2% (JEG-3/VP16,  $p < 0.001$ ) respectively. The  $IC_{50}$  value of resistant cells exposing to chemotherapeutics were decreased with RA dose added (Figure 6e,  $p < 0.05$ ). To further confirmed that RA reversed drug resistance through inducing apoptosis, apoptotic inhibitor Z-VAD-FMK (Selleck, Shanghai, China) was used (Liu et al., 2015). The  $IC_{50}$  value increased apparently which cells treated with 8  $\mu$ M RA and 50  $\mu$ M Z-VAD-FMK together against DMSO group (Figure 6f,  $p < 0.01$ ).

### 3.6 | Raddeanin A-induced apoptosis was STAT3/NFIL3-dependent

To explore the molecular mechanisms underlying RA-mediated apoptosis, we tested if RA can regulate the STAT3/NFIL3 pathway in drug-resistant cells. RA significantly suppressed STAT3 activation and NFIL3 protein expression in each cell lines with dose-dependent manner. But the phenomenon was reversed by STAT3 activator IL-6, suggesting that STAT3/NFIL3 pathway may be involved in RA-mediated apoptosis (Figure 7a). Very obviously, the Caspase 3 inactivated and Bcl-2 expression increased (Figure 7b). Flow cytometry (Figure 7c,  $p < 0.001$ ) and TUNEL (Figure 7d) demonstrated the STAT3 stimulating factor IL-6 abrogated the RA-mediated apoptosis. All these above indicate that the STAT3/NFIL3 axis play a crucial role in RA-inducing apoptosis resisting chemoresistance.

## 4 | DISCUSSION

Preventing and reversing chemoresistance of choriocarcinoma have become one of the focuses of the present studies (Horowitz, Goldstein, & Berkowitz, 2017). For the low-risk choriocarcinoma, methotrexate and fluorouracil are the first-line chemotherapy drugs in choriocarcinoma as monotherapy regimen, and liable to cause resistance. As the most vital regimen for high-risk, relapsing, and resistant choriocarcinoma, EMA-CO regimen involves etoposide which occurs multidrug resistance reported before (Shen et al., 2015). In current study, the JEG-3/MTX, JEG-3/5-FU, and JEG-3/VP16 were used for resistance models. Caspase-cascade is

a central part of cell apoptosis and regulated by various kinds of molecules, such as Bcl-2 family proteins (Fan, Han, Cong, & Liang, 2005; Ghavami et al., 2009). Evidence suggests that some high dosage chemotherapy leads to caspase-independent cell death, but it remains unclear if toxicity to health cells may be a compromising factor in its effectiveness (Su, Yang, Xie, DeWitt, & Chen, 2016). CC cells exhibit intrinsic resistance to chemotherapy drugs, often attributed to high endogenous expression of drug efflux transporters such as MDR1 and some acquired chemoresistance in them develop generations (Ikeda et al., 2012). To combat both intrinsic and acquired chemoresistance, and thus prevent the eventual invincibility of cancer cells, it is important to solve the apoptosis-mediated chemoresistance. We observed the drug-resistant cells showed a low rate of apoptosis contrast to JEG-3 cells. Further the Caspase 3 were activated by chemotherapeutics, including Bcl-2 suppression, which indicated the cell apoptosis pathway. These results hinted us to start with apoptosis issue for solving chemotherapy resistance.

As the survival factor, over-expression of NFIL3 in rat embryonic fibroblasts induced survival genes such as Bcl-2 expression and hindered caspase 3 induction preventing apoptosis (Weng et al., 2010), which was indeed supported by our current finding that NFIL3 expression increased following the cell generations and strikingly related with Caspase 3 dependent apoptosis. In addition, siNFIL3 influenced the  $IC_{50}$  value of the drug-resistant cells, which indicated NFIL3-inhibited apoptosis changed the chemoresistance. This is the first study to evaluate the correlation of NFIL3 and chemoresistance. And the most important what we found was a novel factor influencing choriocarcinoma resistance, which as the potential target for drugs. However, there is no special inhibitor of NFIL3 and short of the direct-bonding compounds.

On the other hand, fortunately, using NCBI database, we learned that the STAT3 possible bind to NFIL3 promoter. Several studies had suggested that IL6/STAT3 pathway was closely associated with the CC cells proliferation (Liu, Gu, & Li, 2013). IL-6 cytokine superfamily-induced activation of STAT3 played a crucial role in induction of invasiveness of trophoblastic cells (Fitzgerald et al., 2005). The expression of p-STAT3 was confirmed related with chemotherapeutic resistance in ovarian, hepatocellular, and neck cancers (Gu et al., 2010; Selvendiran et al., 2009). The drug-resistant JEG-3 cells demonstrated high level of pSTAT3/STAT3 protein expression, which also influenced apoptosis of CC. Besides the direct binding relationship was confirmed in the study, furthermore, down-regulation of STAT3 promoted apoptosis through the suppression of NFIL3, and the activated Caspase 3 were detected. Our results further strengthened the results that anti-apoptotic effect of STAT3 over-expression via regulating NFIL3, and the STAT3/NFIL3 pathway-inhibited apoptosis resulted in chemotherapeutic resistance. But it is worth to mention that, in the observation of three different drug-resistant cells, they showed slightly different results, which maybe there exist disparate resistance mechanism. JEG-3/VP16 cells was detected MDR1 protein expression but JEG-3/MTX and JEG-3/5-FU cells were not (Feng, Xiang, Cui, Liu, & Yang, 2003). JEG-3/MTX showed endoplasmic reticulum stress

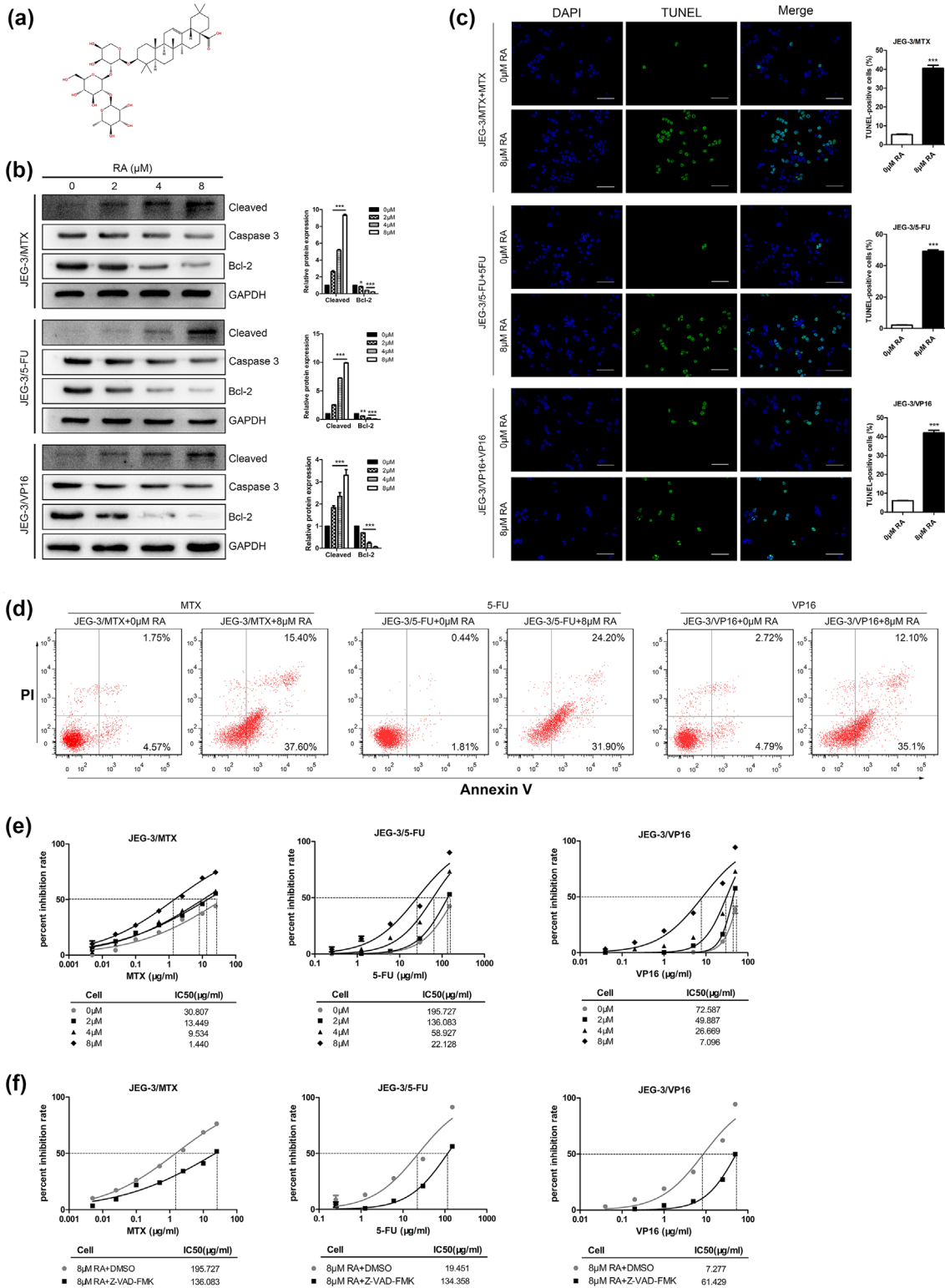


**FIGURE 6** Raddeanin A induced apoptosis to reverse drug resistance. (a) Chemical structure of RA. (b) Cells were treated with RA for 24 hr, and total proteins were extracted. Cleaved-Caspase 3, Caspase 3, and Bcl-2 protein levels analyzed by Western blot. Equal protein loading was evaluated by GAPDH (left). Respective changes in protein levels are depicted as fold change (under). (c) Representative images of TUNEL-stained cells treated with 8 μM RA or not for 24 hr, and then exposed to drugs. Blue DAPI-stained nuclei, green TUNEL-stained positive nuclei, scale bars 100 μm (left). The Respective TUNEL-positive cells are depicted as percent (right). (d) Cells were exposed to chemotherapeutics for 24 hr after Annexin V-FITC/PI staining flow cytometry analysis was performed. (e) IC<sub>50</sub> dose response curves of cells with different doses RA in three sublines. (f) Cells were treated with 8 μM RA for 24 hr, IC<sub>50</sub> dose response curves of cells with 50 μM Z-VAD-FMK in three sublines versus DMSO group. Data represent mean ± SD from at least three independent experiments, \**p* < 0.05, \*\**p* < 0.01, \*\*\**p* < 0.001

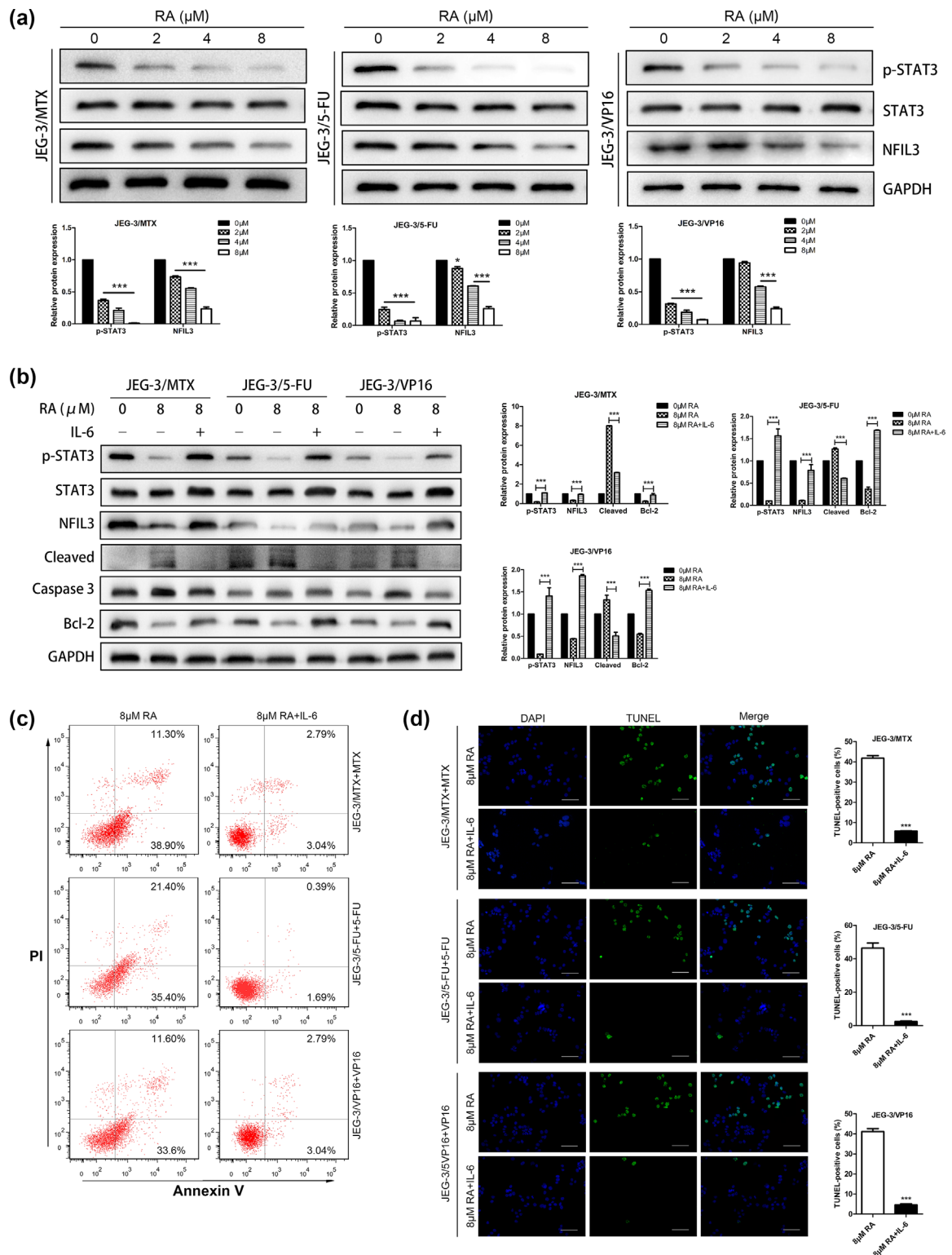


**FIGURE 7** Raddeanin A-induced apoptosis was STAT3/NFIL3-dependent. (a) Cells were treated with RA for 24 hr, and total proteins were extracted. p-STAT3, STAT3, and NFIL3 protein levels analyzed by Western blot. Equal protein loading was evaluated by GAPDH (above). Respective changes in protein levels are depicted as fold change (under). (b) Protein expression levels were analyzed in three cells after 8  $\mu$ M RA with IL-6 (100 ng/ml) treatment or not for 24 hr using Western blots. (c) Cell apoptosis was measured using the flow cytometry 24 hr post RA with IL-6 treatment or not. (d) Representative images of TUNEL-stained cells treated with RA and IL-6 or not for 24 hr, and then exposed to corresponding drugs. Blue DAPI-stained nuclei, green TUNEL-stained positive nuclei, scale bars 100  $\mu$ m. Data represent mean  $\pm$  SD from at least three independent experiments, \* $p < 0.05$ , \*\*\* $p < 0.001$

which induced apoptosis including caspase 9 pathway (Shen et al., 2015). Although further studies are necessary to address the unique resistance mechanism of each resistant cell line, our data allude to a possible mechanism by which STAT3/NFIL3 signaling axis may protect all kinds of drug-resistant cells from apoptosis of chemotherapy drugs.

It is short of big data of choriocarcinoma due to the difficulty in obtaining tissue samples. We analyzed the correlation of STAT3 and NFIL3 in different drug-resistant cells, including colon cancer, breast cancer, malignant melanoma etc. via GEO data. Despite the small sample sizes, the results all indicate the positive correlation of them, further verify our present study. In the predict molecular pathways, we found some interesting molecule related with both STAT3 and NFIL3 directly, such as CREB1 (cAMP responsive element binding protein 1) and NFKBIZ (NFKB inhibitor zeta), which hint that more research can be performed to investigate the regulatory network of STAT3/NFIL3 axis.

Fighting apoptosis is the principal mechanism of tumor cell to resisting death and is an important pointcut for the development of anticancer drugs. In human GC cells, RA can regulate the Bcl-2 family to induce apoptosis (Teng et al., 2016). However, the research on CC cells is still blank. In the present study of CC cells, RA induced apoptosis on both early and late stages via Caspase 3 dependent apoptosis. More importantly, RA reversed the resistance index of resistant cells effectively in dose-dependent manner, which counteracted by Z-VAD-FMAK. Our data now further validate and expand upon the previous findings and provide novel insights into the RA-induced apoptosis controlling the reversal of chemotherapeutic resistance including methotrexate, fluorouracil, and etoposide. Unlike other complementary medicines, RA is more stable in aqueous solution and is less toxic. Low-dose RA used in present study showed effective effect against traditional chemotherapy drugs. Further, we sought to focus our investigation on mechanism in reversal resistance of RA. We observed that RA could repress STAT3 activation and down-regulate NFIL3 expression which mediated by IL-6/STAT3 signaling axis. More importantly, in this study, activated p-STAT3 and NFIL3 could weaken the apoptotic effect of RA, indicating that the activated STAT3/NFIL3 signaling axis results in the changes: loss of apoptosis and chemotherapeutic resistance.

In conclusion, our data support the hypothesis that STAT3/NFIL3 signaling axis-repressed apoptosis is a dominating driving factor responsible for chemotherapeutic resistance, which could be reversed by RA.

## ACKNOWLEDGMENTS

The work was supported by Graduate Independent Innovation Project Fund of Central South University (2016zzts125).

## CONFLICTS OF INTEREST

The authors declare that there are no conflicts of interest.

## ORCID

Yi Zhang  <http://orcid.org/0000-0003-4607-9714>

## REFERENCES

- Chen, Y., Qian, H., Wang, H., Zhang, X., Fu, M., Liang, X., ... Xiang, Y. (2007). Ad-PUMA sensitizes drug-resistant choriocarcinoma cells to chemotherapeutic agents. *Gynecologic Oncology*, 107(3), 505–512.
- Shi, D., Tan, Z., Lu, R., Yang, W., & Zhang, Y. (2014). microRNA-218 inhibits the proliferation of human choriocarcinoma JEG-3 cell line by targeting Fbxw8. *Biochemical and Biophysical Research Communications*, 450(4), 1241–1246.
- Fan, T. J., Han, L. H., Cong, R. S., & Liang, J. (2005). Caspase family proteases and apoptosis. *Acta Biochimica Et Biophysica Sinica*, 37(11), 719–727.
- Feng, F. Z., Xiang, Y., Cui, Z. M., Liu, Z. H., & Yang, X. Y. (2003). In vitro reversal of multidrug resistance by transduction of human tumor necrosis factor- $\alpha$  into drug resistant cell line of choriocarcinoma. *Zhonghua Fu Chan Ke Za Zhi*, 38(5), 294–497.
- Fitzgerald, J. S., Tsareva, S. A., Poehlmann, T. G., Berod, L., Meissner, A., Corvinus, F. M., ... Friedrich, K. (2005). Leukemia inhibitory factor triggers activation of signal transducer and activator of transcription 3, proliferation, invasiveness, and altered protease expression in choriocarcinoma cells. *International Journal of Biochemistry and Cell Biology*, 37(11), 2284–2296.
- Fuchs, Y., & Steller, H. (2011). Programmed cell death in animal development and disease. *Cell*, 147(4), 742–758.
- Ghavami, S., Hashemi, M., Ande, S. R., Yeganeh, B., Xiao, W., Eshraghi, M., ... Los, M. (2009). Apoptosis and cancer: Mutations within caspase genes. *Journal of Medical Genetics*, 46(8), 497–510.
- Gu, F., Ma, Y., Zhang, Z., Zhao, J., Kobayashi, H., Zhang, L., & Fu, L. (2010). Expression of Stat3 and Notch1 is associated with cisplatin resistance in head and neck squamous cell carcinoma. *Oncology Reports*, 23(3), 671–676.
- Guan, Y. Y., Liu, H. J., Luan, X., Xu, J. R., Lu, Q., Liu, Y. R., ... Fang, C. (2015). Raddeanin A, a triterpenoid saponin isolated from *Anemone raddeana*, suppresses the angiogenesis and growth of human colorectal tumor by inhibiting VEGFR2 signaling. *Phytomedicine*, 22(1), 103–110.
- Horowitz, N. S., Goldstein, D. P., & Berkowitz, R. S. (2017). Placental site trophoblastic tumors and epithelioid trophoblastic tumors: Biology, natural history, and treatment modalities. *Gynecologic Oncology*, 144(1), 208–214.
- Ikeda, K., Yamasaki, K., Homemoto, M., Yamaue, S., Ogawa, M., Nakao, E., ... Hirotsani, Y. (2012). Efflux transporter mRNA expression profiles in differentiating JEG-3 human choriocarcinoma cells as a placental transport model. *Pharmazie*, 67(1), 86–90.
- Ikushima, S., Inukai, T., Inaba, T., Nimer, S. D., Cleveland, J. L., & Look, A. T. (1997). Pivotal role for the NFIL3/E4BP4 transcription factor in interleukin 3-mediated survival of pro-B lymphocytes. *Proceedings of the National Academy of Sciences of the United States of America*, 94(6), 2609–2614.
- Kashiwada, M., Pham, N. L., Pewe, L. L., Harty, J. T., & Rothman, P. B. (2011). NFIL3/E4BP4 is a key transcription factor for CD8 $\alpha$ <sup>+</sup> dendritic cell development. *Blood*, 117(23), 6193–6197.
- Li, F., Liu, J., Jo, M., & Curry, T. E., Jr. (2011). A role for nuclear factor interleukin-3 (NFIL3), a critical transcriptional repressor, in down-regulation of periovulatory gene expression. *Molecular Endocrinology*, 25(3), 445–459.
- Li, J. N., Yu, Y., Zhang, Y. F., Li, Z. M., Cai, G. Z., & Gong, J. Y. (2017). Synergy of Raddeanin A and cisplatin induced therapeutic effect enhancement in human hepatocellular carcinoma. *Biochemical and Biophysical Research Communications*, 485(2), 335–341.

- Lim, W., Yang, C., Bazer, F. W., & Song, G. (2017). Chrysophanol induces apoptosis of choriocarcinoma through regulation of ROS and the AKT and ERK1/2 pathways. *Journal of Cellular Physiology*, 232(2), 331–339.
- Liu, X., Gu, W., & Li, X. (2013). HLA-G regulates the invasive properties of JEG-3 choriocarcinoma cells by controlling STAT3 activation. *Placenta*, 34(11), 1044–1052.
- Liu, X. Y., Lai, F., Yan, X. G., Jiang, C. C., Guo, S. T., Wang, C. Y., . . . Zhang, X. D. (2015). RIP1 kinase is an oncogenic driver in melanoma. *Cancer Research*, 75(8), 1736–1748.
- Luan, X., Guan, Y. Y., Wang, C., Zhao, M., Lu, Q., Tang, Y. B., . . . Chen, H. Z. (2013). Determination of Raddeanin A in rat plasma by liquid chromatography-tandem mass spectrometry: Application to a pharmacokinetic study. *Journal of Chromatography B, Analytical Technologies in the Biomedical and Life Sciences*, 923–924, 43–47.
- Lurain, J. R. (2011). Gestational trophoblastic disease II: Classification and management of gestational trophoblastic neoplasia. *American Journal of Obstetrics and Gynecology*, 204(1), 11–18.
- Niu, G., Shain, K. H., Huang, M., Ravi, R., Bedi, A., Dalton, W. S., . . . Yu, H. (2011). Overexpression of a dominant-negative signal transducer and activator of transcription 3 variant in tumor cells leads to production of soluble factors that induce apoptosis and cell cycle arrest. *Cancer Research*, 61(8), 3276–3280.
- Raff, M. C., Barres, B. A., Burne, J. F., Coles, H. S., Ishizaki, Y., & Jacobson, M. D. (1993). Programmed cell death and the control of cell survival: Lessons from the nervous system. *Science*, 262(5134), 695–700.
- Rathore, R., McCallum, J. E., Varghese, E., Florea, A. M., & Büsselberg, D. (2017). Overcoming chemotherapy drug resistance by targeting inhibitors of apoptosis proteins (IAPs). *Apoptosis*, 22(7), 899–919.
- Seckl, M. J., Sebire, N. J., Fisher, R. A., Golfier, F., Massuger, L., & Sessa, C. & ESMO Guidelines Working Group. (2013). Gestational trophoblastic disease: ESMO clinical practice guidelines for diagnosis, treatment and follow-up. *Annals of Oncology*, 24, 39–50.
- Selvendiran, K., Bratasz, A., Kuppasamy, M. L., Tazi, M. F., Rivera, B. K., & Kuppasamy, P. (2009). Hypoxia induces chemoresistance in ovarian cancer cells by activation of signal transducer and activator of transcription 3. *International Journal of Cancer Journal International Du Cancer*, 125(9), 2198–2204.
- Shen, Y., Yang, J., Zhao, J., Xiao, C., Xu, C., & Xiang, Y. (2015). The switch from ER stress-induced apoptosis to autophagy via ROS-mediated JNK/p62 signals: A survival mechanism in methotrexate-resistant choriocarcinoma cells. *Experimental Cell Research*, 334(2), 207–218.
- Smith, A. M., Qualls, J. E., O'Brien, K., Balouzian, L., Johnson, P. F., Schultz-Cherry, S., . . . Murray, P. J. (2011). A distal enhancer in *Il12b* is the target of transcriptional repression by the STAT3 pathway and requires the basic leucine zipper (B-ZIP) protein NFIL3. *The Journal of Biological Chemistry*, 286(26), 23582–23590.
- Snow, K., & Judd, W. (1991). Characterisation of adriamycin- and amsacrine-resistant human leukaemic T cell lines. *British Journal of Cancer*, 63(1), 17–28.
- Su, Z., Yang, Z., Xie, L., DeWitt, J. P., & Chen, Y. (2016). Cancer therapy in the necroptosis era. *Cell Death and Differentiation*, 23(5), 748–756.
- Teng, Y. H., Li, J. P., Liu, S. L., Zou, X., Fang, L. H., Zhou, J. Y., . . . Wang, R. P. (2016). Autophagy protects from Raddeanin A-Induced apoptosis in SGC-7901 human gastric cancer cells. *Evidence-Based Complementary and Alternative Medicine*, 2016, 9406758.
- Turkson, J., & Jove, R. (2000). STAT proteins: Novel molecular targets for cancer drug discovery. *Oncogene*, 19(56), 6613–6626.
- Weng, Y. J., Hsieh, D. J., Kuo, W. W., Lai, T. Y., Hsu, H. H., Tsai, C. H., . . . Tung, K. C. (2010). E4BP4 is a cardiac survival factor and essential for embryonic heart development. *Molecular and Cellular Biochemistry*, 340(1–2), 187–194.
- Xue, G., Zou, X., Zhou, J. Y., Sun, W., Wu, J., Xu, J. L., & Wang, R. P. (2013). Raddeanin A induces human gastric cancer cells apoptosis and inhibits their invasion in vitro. *Biochemical and Biophysical Research Communications*, 439(2), 196–202.
- Yang, Y. P., Chang, Y. L., Huang, P. I., Chiou, G. Y., Tseng, L. M., Chiou, S. H., . . . Chang, C. J. (2012). Resveratrol suppresses tumorigenicity and enhances radiosensitivity in primary glioblastoma tumor initiating cells by inhibiting the STAT3 axis. *Journal of Cellular Physiology*, 227(3), 976–993.
- Yu, H., & Jove, R. (2004). The STATs of cancer-new molecular targets come of age. *Nature Reviews. Cancer*, 4(2), 97–105.
- Zhang, X. M., Zhou, C., Gu, H., Yan, L., & Zhang, G. Y. (2014). Correlation of RKIP, STAT3 and cyclin D1 expression in pathogenesis of gastric cancer. *International Journal of Clinical and Experimental Pathology*, 7(9), 5902–5908.

## SUPPORTING INFORMATION

Additional Supporting Information may be found online in the supporting information tab for this article.

**How to cite this article:** Peng Z, Zhang C, Zhou W, Wu C, Zhang Y. The STAT3/NFIL3 signaling axis-mediated chemotherapy resistance is reversed by Raddeanin A via inducing apoptosis in choriocarcinoma cells. *J Cell Physiol*. 2018;233:5370–5382. <https://doi.org/10.1002/jcp.26362>